

See discussions, stats, and author profiles for this publication at: <http://www.researchgate.net/publication/276363987>

Immobilizing Systems Biocatalysis for the Selective Oxidation of Glycerol Coupled to In Situ Cofactor Recycling and Hydrogen Peroxide Elimination

ARTICLE *in* CHEMCATCHEM · MAY 2015

Impact Factor: 5.04 · DOI: 10.1002/cctc.201500210

DOWNLOADS

21

VIEWS

38

4 AUTHORS, INCLUDING:



Javier Rocha Martín

Abengoa

22 PUBLICATIONS 221 CITATIONS

SEE PROFILE



Jose M Guisan

Spanish National Research Council

438 PUBLICATIONS 10,603 CITATIONS

SEE PROFILE



Fernando López-Gallego

CIC biomaGUNE

72 PUBLICATIONS 1,639 CITATIONS

SEE PROFILE

Immobilizing Systems Biocatalysis for the Selective Oxidation of Glycerol Coupled to In Situ Cofactor Recycling and Hydrogen Peroxide Elimination

Javier Rocha-Martin,^[c, d] Andreína Acosta,^[d] Jose M. Guisan,^{*,[d]} and Fernando López-Gallego^{*,[a, b]}

The combination of three different enzymes immobilized rationally on the same heterofunctional carrier allowed the selective oxidation of glycerol to 1,3-dihydroxyacetone (DHA) coupled to in situ redox-cofactor recycling and H₂O₂ elimination. In this cascade, engineered glycerol dehydrogenase with reduced product inhibition oxidized glycerol selectively to DHA with the concomitant reduction of NAD⁺ to NADH. NADH oxidase regenerated the NAD⁺ pool by oxidizing NADH to NAD⁺ to form H₂O₂ as the byproduct. Finally, catalase eliminated H₂O₂

to yield water and O₂ as innocuous products, which avoided the spontaneous DHA oxidation triggered by H₂O₂. The co-immobilization of the three enzymes on the same porous carrier allowed the in situ recycling and disproportionation of the redox cofactor and H₂O₂, respectively, to produce up to 9.5 mM DHA, which is 18- and 6-fold higher than glycerol dehydrogenase itself and a soluble multienzyme system, respectively.

Introduction

The construction of synthetic chemical cascades with multienzyme systems is gaining popularity because they can catalyze chemical reactions selectively under mild conditions.^[1] Enzymes have evolved their properties over thousands of millions of years to catalyze an immense diversity of chemical reactions efficiently inside the same bioreactor—the cell—and in the same reaction media—cytoplasm. Inside this living vessel, different enzyme activities must work as an orchestra that is tuned perfectly to coordinate and regulate the chemical fluxes through the metabolic network that sustains the cell life. In the last decade, chemists have been delighted by such catalytic orchestration found in vivo and have isolated multienzyme systems to work ex vivo in both natural and non-natural tandem reactions to create a new concept: systems biocatalysis.^[1–3] These systems are pioneers of cell-free synthetic biology,

an emerging discipline that seeks the simplest biology to make the most complex chemistry.

However, enzymes often have disadvantages for industrial applications because they present some properties that do not meet the requirements imposed by the chemical processes in industry. For this reason, scientists have devoted enormous efforts to engineer enzymes to overcome their limitations as industrial catalysts. With this aim, protein engineering has been shown as one of the most effective approaches to adapt enzymes to industrial requirements.^[4,5] Nevertheless, the protein engineering approach cannot address the solubility issue of enzymes that hampers their reusability and workability in flow processes. Hence, protein immobilization appears as a complementary approach to protein engineering to make enzymes suitable for the chemical industry.^[6,7] The immobilization of an enzyme onto a solid carrier simplifies the downstream processing, and if the immobilization procedure is well designed, immobilization also guarantees the stability and, consequently, the reusability of the biocatalyst. Enzyme immobilization may also improve other enzyme properties such as activity, selectivity, or inhibition.^[8] In the last decade, several strategies have been developed to merge protein engineering and protein immobilization synergistically to create heterogeneous biocatalysts with improved properties.^[6,9]

We have paid attention to the preparation of immobilized multienzyme systems to catalyze tandem reactions.^[10–12] The co-immobilization of multienzyme systems can improve: 1) the kinetics of the chemical cascade because of the spatial localization of the different biocatalytic modules, which avoids the accumulation of intermediates and increases the cofactor recycling efficiency^[10] and 2) the stability of the biocatalyst because of the in situ elimination of toxic byproducts.^[13] Nevertheless,

[a] Dr. F. López-Gallego
Department Biofunctional nanomaterials unit. CIC BiomaGUNE
Pase Miramon 182, 20009, San Sebastián-Donostia (Spain)
E-mail: flopez.ikerbasque@cicbiomagune.es

[b] Dr. F. López-Gallego
IKERBASQUE, Basque Foundation for Science
Bilbao (Spain)

[c] Dr. J. Rocha-Martin
BIOMERIT Research Centre, School of Microbiology
University College Cork
National University of Ireland
Cork (Ireland)

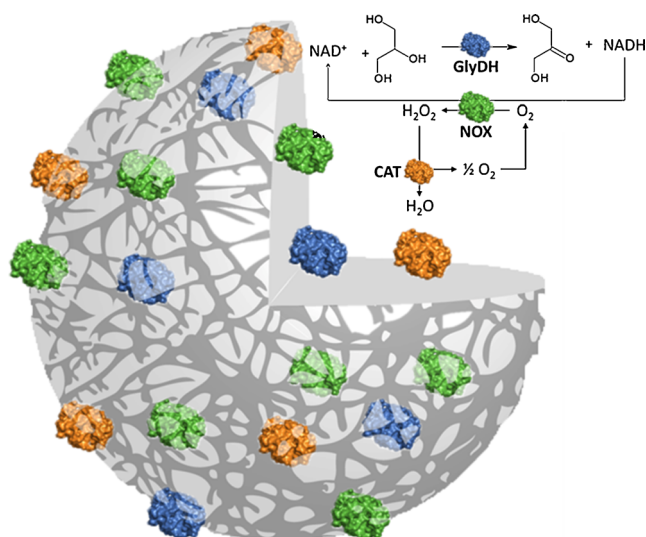
[d] Dr. J. Rocha-Martin, A. Acosta, Prof. J. M. Guisan
Departamento de Biotransformación, Instituto de Catálisis y Petroleoquímica-CSIC
Campus UAM. Cantoblanco, 28049 Madrid (Spain)
E-mail: jmguisan@icp.csic.es

Supporting Information for this article is available on the WWW under
<http://dx.doi.org/10.1002/cctc.201500210>.

the co-immobilization of several enzymes to form a multienzyme system is challenging because there is not a universal immobilization chemistry that can optimally attach all the enzymes to the same surface. In this context, the immobilization chemistry for each enzyme must be selected to preserve, or ideally to improve, the enzyme properties (e.g., activity, stability, product inhibition). The fabrication of a heterofunctional carrier activated with different reactive groups that enable different immobilization chemistries^[14] has allowed us to coordinate the immobilization of several enzymes on the same surface. We have recently reported two examples in which the optimal design of the immobilization protocols allowed the co-immobilization of several enzymes on the same carrier through their optimal immobilization chemistries, which preserved both the global activity and stability of the multienzyme systems.^[10,13] The success of this approach relies on the versatility of the surface chemistry given by the agarose beads that allows us to synthesize carrier surfaces activated with different reactive groups that specifically attach each enzyme through its optimal immobilization chemistry.

The selective oxidation of glycerol to yield 1,3-dihydroxyacetone (DHA) is an industrially relevant process because DHA is a valuable chemical with a wide range of applications in fine chemistry with a market price 100 times higher than that of glycerol.^[15,16] DHA synthesis catalyzed by isolated glycerol dehydrogenase is rather limited by product inhibition suffered by such enzymes. Furthermore, the enzymatic synthesis of DHA requires expensive redox cofactors that burden the industrial application of this biotransformation. This issue has been addressed extensively by the incorporation of a recycling system for the redox cofactor into the biotransformation.^[17] A strategy used widely to replenish the NAD⁺ pool enzymatically is the use of H₂O₂-producing NADH oxidase, which only requires O₂ as the oxidant. However, the NADH oxidase must be coupled to a catalase that catalyzes H₂O₂ disproportionation to water and O₂ to avoid enzyme inactivation and unspecific product oxidation caused by H₂O₂.^[18]

In this work, we report the development of an immobilized trienzyme system that catalyzes an orthogonal reaction cascade to oxidize glycerol selectively to DHA with both in situ redox-cofactor recycling and toxic byproduct elimination (Scheme 1). Firstly, we engineered glycerol dehydrogenase to minimize its product inhibition, which impacted positively on the final DHA yield. Then, the three enzymes were optimally immobilized on agarose beads activated heterogeneously with both aldehyde and amine groups. The amine groups enable the ionic absorption of enzymes under pH 7, and the glyoxyl groups promote their multipoint covalent attachment under alkaline conditions. Furthermore, the multimeric character of three enzymes that form the multienzyme system led us to use post-immobilization chemical modification with dextran aldehydes to increase the stability and reduce the product inhibition of the supported cell-free system.



Scheme 1. Immobilized multienzyme system for glycerol oxidation with both in situ NAD⁺ recycling and H₂O₂ elimination.

Results and Discussion

Bio-oxidation of glycerol to DHA catalyzed by a soluble trienzyme system

We have designed a trienzyme cascade to oxidize glycerol into DHA with in situ redox-cofactor recycling and without using a sacrificial substrate (Scheme 1). In this cascade, glycerol dehydrogenase (GlyDH) from *Geobacillus stearothermophilus*^[19] oxidizes glycerol selectively to DHA and reduces NAD⁺ concomitantly to NADH. Then, NADH oxidase (NOX) from *Thermus thermophilus*^[20]—a flavoprotein—regenerates the NAD⁺ pool by oxidizing NADH to NAD⁺ using oxygen as the electron acceptor, which results in the formation of H₂O₂ as the byproduct. Finally, the H₂O₂ is eliminated by the catalase from bovine liver (CAT)^[21] to yield water and O₂ as innocuous products, which avoids the potential side oxidation reactions triggered by H₂O₂. Moreover, the O₂ produced from the H₂O₂ elimination enters the NAD⁺ regeneration cycle. Therefore, in this orthogonal enzyme cascade, O₂ is used indirectly to oxidize glycerol to yield DHA and water as products.

In multienzyme systems, it is important to orchestrate the catalytic activity of each enzyme to achieve the correct performance of the reaction cascade. With this aim, we have studied different activity ratios of each biocatalyst. First, we tested the optimal activity ratio between GlyDH and NOX. NOX/GlyDH activity ratios of 4–10 resulted in a similar DHA yield (8%), whereas the reaction without NOX only reached a maximum DHA yield of 5% (Figure 1A). Similar results were observed if the GlyDH from *Escherichia coli* was coupled to NOX from *Bacillus cereus* to produce 4-hydroxy-2-butanone from 1,3-butanediol.^[22] We also tested different CAT/GlyDH ratios with a constant NOX/GlyDH ratio of 4. A CAT/GlyDH ratio between 250 and 1000 achieved 12% of the DHA theoretical yield (Figure 1B), whereas the multienzyme system that lacked CAT was able to produce only 8% of the DHA theoretical yield. Hence, we conclude that the CAT/GlyDH ratio must be higher

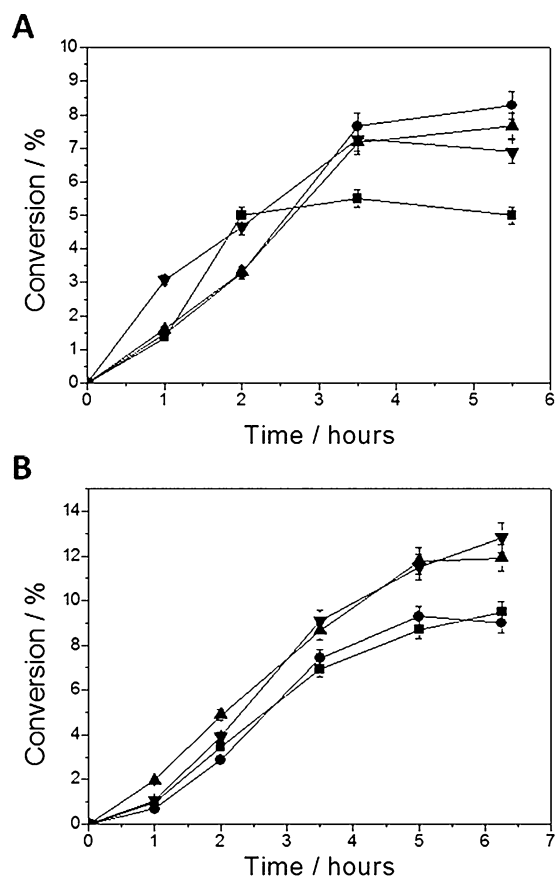


Figure 1. Influence of A) NOX and B) CAT excess on the biotransformation efficiency. Reactions were performed at 25 °C in 5 mL of 100 mM potassium phosphate pH 7, 10 mM glycerol, 0.5 mM NAD⁺, and 0.5 mM flavin mononucleotide. The reactions were triggered with 1 U of wild-type GlyDH. In A), the NOX activity was varied from 0 (■), 2 (▲), 4 (●), and 10 IU (▼) in the absence of CAT. In B), NOX was constant at 4 IU, and the CAT activity varied from 0 (■), 10 (●), 250 (▲), and 1000 IU (▼).

than the NOX/GlyDH ratio to achieve a high titer of DHA. In light of these results, we used a trienzyme system with an optimal activity with a CAT/NOX/GlyDH ratio of 250:4:1. In this scenario, the DHA yield is enhanced mainly because of a higher availability of NAD⁺ provided by the action of NOX and the absence of H₂O₂ as result of the activity of CAT.

The positive impact of the in situ NAD⁺ recycling on the system productivity was also demonstrated with other glycerol dehydrogenases using xylose reductase instead of NOX as the recycling enzyme.^[23] The in situ elimination of H₂O₂ avoids the spontaneous oxidation of DHA to glycolic acid, which reduces the final product yield.^[24] Finally, the three enzymes were compatible in potassium phosphate buffer at pH 7, hence it is possible to perform this biotransformation in one pot and in aqueous media.

In spite of the improvement in the final yield provided by the cooperation of cofactor recycling and H₂O₂ elimination, the DHA concentration was never higher than 1.5 mM, which is less than 15% of the theoretical yield. Such a low product yield is because of the strong product inhibition by GlyDH. Therefore, this inhibition is the limiting step of this multien-

zyme process. A similar inhibitory effect was observed for GlyDH from *Cellulomonas sp.* and *Citrobacter braaki*.^[25,26] Kinetics studies have revealed that DHA causes a noncompetitive inhibition on the GlyDH from *Geobacillus stearothermophilus*.^[27]

Reduction of DHA inhibition by engineering GlyDH

The X-ray structure and some kinetics studies of GlyDH from *Geobacillus stearothermophilus* (PDB code 1JQA)^[27] enabled us to predict rationally some potential residues involved in the DHA binding. As well as other multimeric enzymes, we presume that GlyDH undergoes allosteric inhibition, although little is known about its allosteric site and its molecular mechanism. In the last decade, several groups have made use of the COREX/BEST algorithm to predict the allosteric regulation of proteins based on structural information.^[28] Aided by this algorithm, we can propose flexible regions on the protein structure as potential binding sites for allosteric inhibitors. Such regions will become rigid once the inhibitor binds to them. As allostery relies on protein dynamics,^[29] we have engineered flexible regions to block inhibition.

Some flexible residues in the surroundings of the GlyDH active center are highlighted in Figure 2A but they are involved in neither the substrate binding nor the catalytic mechanism. H271, H270, E268, and K97 residues presented low stability factors after COREX/BEST analysis, which indicates that they are very flexible. This flexibility might indicate that such a region is prone to conformational changes triggered either by the substrate (glycerol) or by the inhibitor (DHA) that facilitates the catalysis or the inhibition, respectively. Moreover, Ruzheinkov et al. have suggested that H271 interacts with a Zn atom (as the structure reveals) that may establish an intermolecular interaction with H270 from other octamers, which affects the final activity of the biocatalyst.^[19] These insights support the possible role of this area in the allosteric inhibition triggered by DHA. To demonstrate such a hypothesis, we made five different single mutants, K22Q, K97Q, E268Q, H270P, and H271P, with the aim to eliminate any electrostatic, van der Waals, hydrophobic, and hydrogen bond interactions between these residues and DHA.

The specific activity and the half maximal inhibitory concentration (IC₅₀) towards DHA of each single mutant is given in Table 1.

Table 1. Specific activity and IC₅₀ of the different mutants constructed.^[a]

	Specific activity [U mg ⁻¹]	IC ₅₀ DHA [mM]
Wild type	70	0.67
K22Q	nd	nd
K97Q	0.7	3
E268Q	17.8	0.45
H270P	12.7	1
H271P	70	1

[a] IC₅₀ is the DHA concentration that inhibits 50% of enzyme activity. Specific activity measured at pH 8 and 25 °C. nd: not detected.

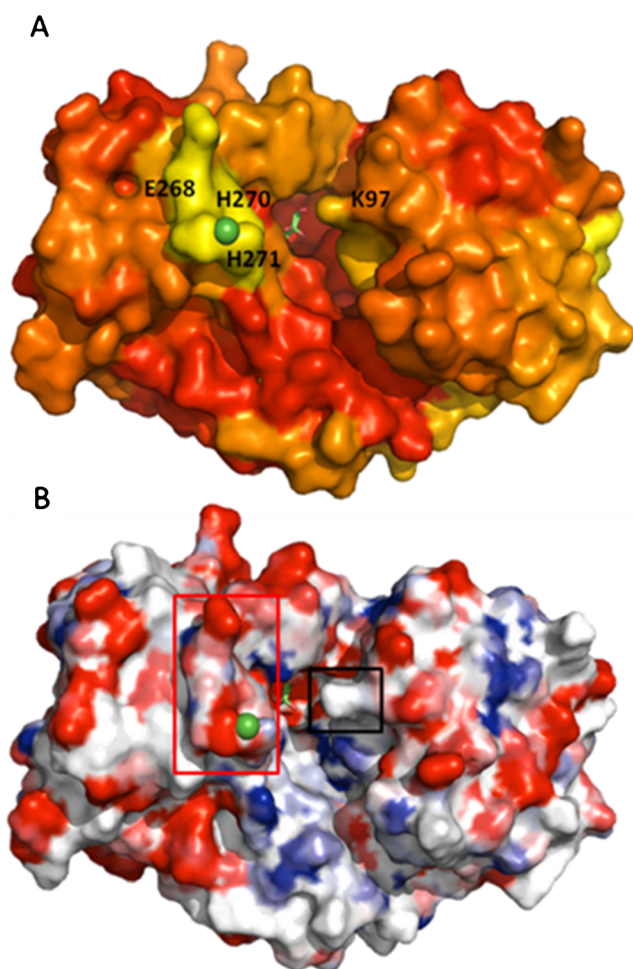


Figure 2. A) In silico representation of the local flexibility of GlyDH-Gs by using the COREX/BEST server. Rigid and flexible residues are colored in red and orange, respectively. Shades intermediate between red and yellow represent moderately stable regions. Residues E266-H271 (orange) present a moderate flexibility and are located at the enzyme C terminus domain. B) Electrostatic surface potential. Red color represents negatively charged residues, and blue color represents positively charged residues. The figure was created with pymol 0.99 (DeLano, USA) using the PDB ID: 1 JQA. The electrostatic potential was calculated by using the Blues server.^[31]

The mutant K22Q was the unique fully inactive mutant. For the other mutants, we observed lower specific activities than the wild type although they were inhibited differently by DHA. Although K97Q diminished the product inhibition by a factor of 4.5, mutant E268Q presented a higher inhibition than the wild type. Paradoxically, the mutant that minimizes the DHA inhibition the most: K97Q, expressed the lowest specific activity; only 1% of the wild-type specific activity. This dramatic reduction in enzyme activity may be because of the important catalytic role of K97 although it is not located at the glycerol binding pocket.^[30] Paine et al. reported that the mutant K97H was fully inactive and suggested that such a residue was crucial for NADH binding.^[30] However, in the mutant K97Q, we could measure enzyme activity that clearly minimized the product inhibition, which indicates that GlyDH-K97Q still binds the redox cofactor but hinders DHA binding. According to the electrostatic surface potential calculated from the Poisson–Boltzmann

equation,^[31] the ϵ -NH₂ group of K97 is mostly deprotonated (Figure 2B). Such an electronic state of lysine 97 may favor the nucleophilic attack of the amine group on the carbonyl group of DHA. This is supported by a previous study that has reported the specific interaction between the same residue of the GlyDH from *Geobacillus stearothermophilus* and the aldehyde group of pyridoxal-5-phosphate.^[30] This interaction blocks the entry of glycerol to the active center and, therefore, inactivates the enzyme as DHA would do.

These kinetics and structural insights are observed during the operation process catalyzed by the trienzyme system. The wild-type enzyme and the GlyDH-K97Q variant were coupled to NOX and CAT to oxidize glycerol selectively to DHA with in situ cofactor regeneration and H₂O₂ elimination. The soluble multienzyme system with the GlyDH-K97Q variant yielded up to 2.5 mM DHA in 7 h, whereas the wild-type enzyme could only produce 1.25 mM DHA over the same time interval (Figure 3). Moreover, the maximum production rate of the en-

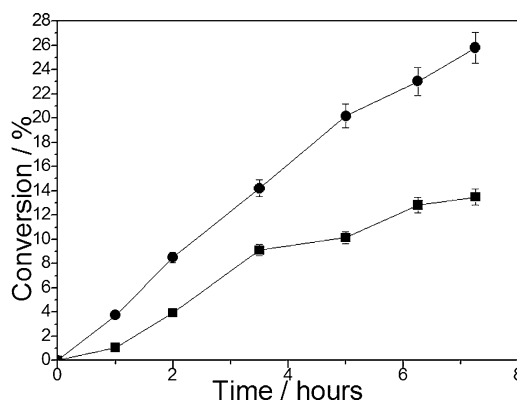


Figure 3. Glycerol oxidation catalyzed by soluble wild-type (■) and K97Q (●) variants of GlyDH. Reactions were performed at 25 °C in 100 mM potassium phosphate pH 7, 10 mM glycerol, 0.5 mM NAD⁺, and 0.5 mM flavin mononucleotide. GlyDH (2 U), NOX (4 U), and CAT (1000 U) of soluble enzymes were added to 5 mL of reaction volume.

gineered system was 0.4 mm h⁻¹, which is 180% higher than the system that contains the wild-type enzyme. Therefore, in silico studies of the protein surface have helped us to propose one residue that seems to be involved in DHA binding. The directed mutagenesis of this site resulted in an engineered variant that is less sensitive to DHA concentration.

The effect of immobilization and covalent crosslinking on the performance of the trienzyme system

Recently, we reported that the immobilization of GlyDH from *Geobacillus stearothermophilus* on agarose beads activated with both amine and glyoxyl groups (Ag-AG) and its further covalent crosslinking with dextran aldehyde reduces the DHA product inhibition by a factor of six with regard to the soluble enzyme.^[27] Both NOX and CAT were also immobilized individually on Ag-AG and further crosslinked with the same functional dextran polymer. The resulting insoluble and crosslinked preparations were used to oxidize glycerol with in situ NAD⁺ recy-

cling and H₂O₂ elimination. Notably, the reactions catalyzed by soluble wild-type GlyDH, NOX, and CAT only reached 1.25 mM of DHA with a production rate of 0.2 mm h⁻¹ (Figure S1), whereas the same enzymes immobilized separately on Ag-AG and further crosslinked with dextran aldehyde produced DHA 2.4 times more rapidly (Figure S1) to reach a final yield two times higher (2.8 mM) (Figure 4). This result motivated us to

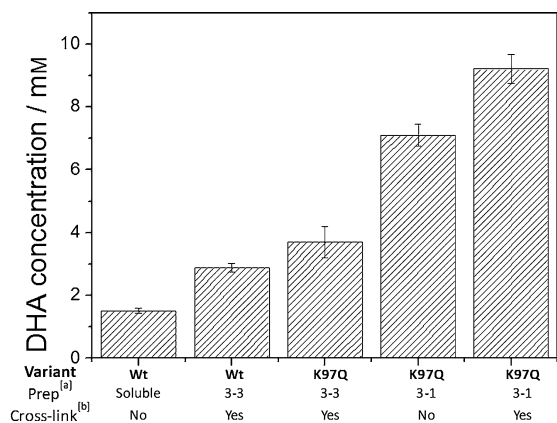


Figure 4. DHA titer [mM] after glycerol biotransformation catalyzed by different multienzyme systems (soluble and immobilized). [a] Biocat 3-3 means that NOX, CAT, and GlyDH are immobilized separately on three different carriers. Biocat 3-1 means that NOX, CAT, and GlyDH are co-immobilized on the same carrier. [b] Crosslinking was performed in a post-immobilization stage by using dextran polymers activated with aldehyde groups. Reactions were stopped after 9 h, and the product yield was analyzed.

immobilize covalently and crosslink the engineered GlyDH-K97Q variant on Ag-AG under the optimal conditions we established previously. The combination of such insoluble and crosslinked engineered GlyDH with the immobilized NOX and CAT yielded up to 3.7 mM of DHA, which is 1.3 times higher than the system formed by wild-type GlyDH (Figure 4). However, the production rates of both systems were quite similar. This result demonstrates that engineered GlyDH-K97Q minimized DHA inhibition to increase the final product yield. Moreover, the mutant GlyDH was also stabilized by such immobilization and crosslinking chemistry as well as the wild-type variant reported recently by our group (Figure S2).^[27] Likewise, we have already reported that multipoint covalent immobilization and crosslinking through aldehyde chemistry stabilizes both NOX and CAT.^[32,33]

Therefore, the immobilization of such a trienzyme system on Ag-AG minimizes product inhibition and maximizes protein stability. On one hand, as GlyDH, NOX, and CAT are multimers, their post-immobilization covalent crosslinking avoids subunit dissociation, which stabilizes their quaternary structures.^[34] On the other hand, the immobilization of GlyDH on the Ag-AG carrier seems to be optimal to minimize the product inhibition suffered by this enzyme.^[27] Hence, by merging immobilization and protein engineering we have managed to reduce the inhibition of GlyDH by DHA and increase the thermal stability of all the enzymes that participate in the biotransformation simultaneously.

Co-immobilization and further crosslinking of the trienzyme system on Ag-AG: Improving the production rate, yield, and in situ elimination of H₂O₂

GlyDH-K97Q, NOX, and CAT were co-immobilized sequentially on the Ag-AG carrier. Firstly, GlyDH-K97Q was absorbed ionically onto the carrier at pH 7 through the amino groups present on the Ag-AG surface, then CAT was immobilized covalently at pH 10 through the aldehyde groups on the Ag-AG surface, and finally NOX was immobilized covalently under the same conditions as CAT, and thereby through the same chemistry. Furthermore, GlyDH-K97Q absorbed ionically was also attached covalently to the carrier surface as a consequence of the alkaline incubation that promoted the immobilization of the other two enzymes.

This immobilization sequence was optimal to ensure both the maximum expressed activity and the highest stability for each enzyme after the immobilization (Table S1). The catalytic loading of the final insoluble biocatalyst that bears the three enzymes followed the optimal activity ratio of 250:4:1 (CAT/NOX/GlyDH). As we described previously, this ratio led to the highest DHA yield if the soluble enzymes were used.

The co-immobilized multienzyme system was tested for the bio-oxidation of glycerol and compared with the multienzyme system in which each enzyme was immobilized separately on different carriers. The progress of the glycerol oxidation reaction with time catalyzed by the different immobilized preparations of this trienzyme system is shown in Figure S3. The co-immobilization of the three enzymes on one carrier (biocat 3-1) oxidized glycerol twice as rapidly and yielded a 1.9 times higher product titer than the system in which the three enzymes were immobilized separately on three carriers (biocat 3-3; Figure 4 and Figure S3). The in situ elimination of H₂O₂ generates O₂ within the microstructure of the carrier particles, which may boost the NAD⁺ recycling because it would increase the intraparticle O₂ concentration to accelerate NOX. In this context, we suggest that the higher DHA production rate with the co-immobilized system relies on the enhancement in the cofactor recycling frequency.

Additionally, biocat 3-1 was crosslinked with dextran aldehyde after the sequential immobilization of the three enzymes. This covalent crosslinking led the co-immobilized biocatalyst to yield up to 9.22 mM DHA; almost 50% of the theoretical yield. As far as we know, this is the highest yield ever reported for DHA production catalyzed by any isolated GlyDH both in its soluble and immobilized forms.^[23,35] Interestingly, this observed improvement was only because of the colocalization of the three enzymes within the same porous environment, because in both biocatalysts (biocat 3-1 and biocat 3-3) the chemical interactions between each enzyme and the carrier surface were exactly the same. We studied the efficiency of the different immobilized biocatalysts to eliminate the H₂O₂ concomitantly formed from the NADH enzymatic oxidation (Table 2) and we observed that NADH was oxidized quantitatively by using immobilized NOX to accumulate 140 μM of H₂O₂, which is 56% of the theoretical maximum conversion. We never observed 100% NADH conversion, which is likely be-

Table 2. Efficiency of the different immobilized biocatalysts to eliminate the H₂O₂ concomitantly formed from the enzymatic reduction of NAD⁺.

Biocatalyst	[H ₂ O ₂] in bulk [μM]	Efficiency of H ₂ O ₂ elimination [%]
Ag-AG-NOX	140	–
Biocat 3-3 ^[a]	19	86
Biocat 3-1 ^[b]	2	99

[a] Biocat 3-3: NOX and CAT are immobilized separately on two different carriers. [b] Biocat 3-1: NOX and CAT are co-immobilized on the same carrier. [c] If we consider 100% of H₂O₂ is the concentration of H₂O₂ produced and detected in the enzymatic reaction performed by NOX immobilized on Ag-AG and further crosslinking with dexCHO. See Experimental Section.

cause some of the H₂O₂ was decomposed spontaneously. Therefore, accumulation values might be underestimated because of the indirect method we used to titer H₂O₂ (see Experimental Section). However, NOX and CAT immobilized separately on two different carriers oxidized NADH quantitatively to accumulate 19 μM H₂O₂; 7.3% of its theoretical yield. This means that CAT partially eliminated the H₂O₂. Nevertheless, we only detected 2 μM of H₂O₂ in the quantitative NADH oxidation catalyzed by NOX and CAT co-immobilized on the same carrier. Such a residual H₂O₂ concentration is 0–1% of the theoretical yield. Hence, the colocalization of NOX and CAT accumulate negligible H₂O₂ in the bulk solution as the levels of H₂O₂ detected are quite close to the detection limit of the colorimetric assay. These results indicate that immobilized CAT is able to eliminate H₂O₂ in situ and it does this more efficiently if it is co-immobilized with NOX on the same carrier porous surface.

The success of this co-immobilized and co-crosslinked engineered biocatalyst is driven by the synergy between the immobilization and post-immobilization chemistry that reduces the product inhibition of GlyDH and co-immobilization of the three enzymes that enable their spatial colocalization within the porous carriers. Such a spatial localization of the immobilized multienzyme system improves both the yield and kinetics of the biotransformation. This improvement is mainly because both NAD⁺ recycling and H₂O₂ elimination are much more rapid and efficient in the porous microenvironment. The better performance of these two processes causes a higher effective concentration of NAD⁺ available for the glycerol oxidation and an undetectable H₂O₂ concentration accumulated inside the pores. As expected, the higher effective NAD⁺ concentration improved the total turnover number (TTN) of the system up to 20. The TTN values were not as high as those reported for other multienzyme cascades that involve orthogonal redox-cofactor recycling.^[36] The TTN numbers are low probably because in this multienzyme cascade the limiting step is the product inhibition of GlyDH rather than the NAD⁺ recycling. The observed TTN values for the co-immobilized system are comparable to those reported for DHA production catalyzed by GlyDH from *Cellulomonas sp* and Xylose reductase from *Pichia stipitis* immobilized on silica nanoparticles and GlyDH^[23] from *Citrobacter braakii* and NOX from *Thermus thermophilus* co-immobilized on agarose beads^[10] under similar conditions. Moreover,

the complete elimination of H₂O₂ avoids enzyme inactivation by chemical oxidation and, importantly, avoids the unspecific oxidation of DHA that reduces the product yield of the biotransformation dramatically.^[24] The action of both NOX and CAT recycles and eliminates the redox cofactor and the peroxide in situ, respectively, within the same porous microenvironment, which increases both the kinetics and yield of the DHA biosynthesis.

This new heterogeneous multienzyme system resulted in a four times higher glycerol conversion to DHA than the multienzyme system formed by GlyDH from *Cellulomonas sp* co-immobilized with Xylitol reductase on silica nanoparticles.^[23] Furthermore, this trienzyme immobilized biocatalyst reaches even higher DHA yields than those found for other 2-hydroxyketones, such as 4-hydroxy-2-butanone and 2-hydroxycyclohexanone.^[25] Therefore, the rational integration of protein engineering and immobilization techniques has resulted in immobilized multienzyme systems with better properties to yield DHA by the selective oxidation of glycerol.

Conclusions

A supported cell-free platform based on a trienzyme system, glycerol dehydrogenase (GlyDH), NADH oxidase, and the catalase from bovine liver, was designed and tested for the selective oxidation of glycerol to 1,3-dihydroxyacetone with both in situ redox-cofactor recycling and H₂O₂ elimination. Firstly, we engineered GlyDH to minimize its product inhibition that led to poor yields. The product inhibition of this enzyme was improved by at least five times by combining protein engineering and immobilization techniques. The engineered GlyDH was co-immobilized with the other two enzymes, which confined them into the same micrometric and porous environment. As result of such confinement, the heterogeneous biocatalyst produced up to 9.5 mM 1,3-dihydroxyacetone, which is 18- and 6-fold higher than glycerol dehydrogenase itself and the soluble multienzyme system, respectively. Moreover the co-immobilized multienzyme system presented a 4.5 times higher productivity and eliminated the H₂O₂ formed during the NAD⁺ recycling quantitatively. Therefore, this work demonstrates, once more, that the interdisciplinary engineering of biocatalysts results in integral solutions to overcome process bottlenecks. This biocatalyst opens new opportunities for process engineering to scale up the process under the best reaction conditions.

Experimental Section

Chemicals

NAD⁺ and NADH were purchased from GERBU Biotechnik GmbH (Wieblingen, Germany). Glycidol, glycerol, triethylamine (TEA), polyethylene glycol (PEG), sodium borohydride, sodium periodate, peroxidase from horseradish (HRP), and SIGMAFAST DAB (3,3'-diaminobenzidine tetrahydrochloride) with Metal Enhancer Tablet Sets (DAB) were supplied by Sigma-Aldrich (St. Louis, IL). DHA was supplied by Acros Organics (Geel, Belgium). Crosslinked agarose beads (4%) were from Agarose Beads Technology (Madrid, Spain). The Coomassie (Bradford) protein assay kit was purchased from Pierce

(Rockford, Illinois, USA). All other used reagents were of analytical grade.

Preparation of the different agarose supports

Monoaminoethyl-*N*-aminoethyl agarose (Ag-MANAE) activated partially used for the GlyDH-Gs purification was prepared as described previously.^[37] Agarose beads activated with glyoxyl groups (Ag-G) and agarose beads activated with both amine and glyoxyl groups (Ag-AG) were prepared as described previously in Ref. [27].

Cloning of glycerol dehydrogenase variants from *Geobacillus stearothermophilus* (GlyDH)

Bacterial strains and growth conditions

Laboratory stocks of *Escherichia coli* DH5 α and BL21 (DE3) strains were used to produce chemically competent bacteria that were used for cloning and expression purposes, respectively. *E. coli* strains were cultured aerobically in Luria-Bertani (LB) medium at 37 °C. To overexpress the glycerol dehydrogenase from *G. Stearothermophilus*, we used the plasmid pET28b-glydh described previously.^[27]

Site-directed mutagenesis to create the variants of GlyDH

A site-directed mutagenesis protocol was used to construct five GlyDH mutants (K22Q, K97Q, E268Q, H270P, and H271P). These mutants were made by using the native *glydh* gene as the template. Briefly, to introduce the amino acid change, the corresponding pair of oligonucleotides (Table S2) was used as a primer pair in a polymerase chain reaction (PCR) using a specific plasmid as the template and Prime Start HS Takara DNA polymerase. The product of the PCR was digested with DpnI that exclusively restricts methylated DNA. *E. coli* DH5 α cells were transformed directly with the digested product. The plasmids that bear the mutated *glydh* genes were identified by sequencing and then they were transformed into *E. coli* BL21(DE3) cells to express the corresponding proteins.

Production of the recombinant GlyDH in *E. coli*

E. coli BL21 (DE3) cells were transformed with the recombinant plasmid pET28b-GlyDH. Cells that contained the plasmid were grown at 37 °C in LB medium supplemented with kanamycin (50 $\mu\text{g mL}^{-1}$) and induced by the addition of 1 mM isopropyl-1-thio- β -D-galactopyranoside (IPTG) when the culture reached OD₆₀₀ = 0.5. After 4 h at 37 °C, the cells were collected by centrifugation (10000 $\times g$, 10 min).

Purification of the GlyDH

For protein purification, harvested cells were resuspended in purification buffer (5 mM sodium phosphate at pH 7.0). The cells were lysed by sonication, and the extract was centrifuged at 12000 rpm to remove the cell debris. The resulting soluble crude extract was subjected to anion-exchange chromatography in Ag-MANAE equilibrated with the purification buffer. Following the protein binding, the column was washed three times with purification buffer before elution with NaCl solution (300 mM).

Enzymatic activity assays

The activities of the different GlyDH preparations was analyzed spectrophotometrically by recording the increment of absorbance at $\lambda = 340 \text{ nm}$ ($\epsilon_{\text{NADH}} = 6.22 \text{ mm}^{-1} \text{ cm}^{-1}$) promoted by the formation of NADH during the oxidation of glycerol. A sample of enzymatic preparation (10–200 μL) was added to a cell with 2 mL of 100 mM glycerol and 50 μL of 100 mM NAD⁺ in 100 mM sodium phosphate at pH 7.0 at 25 °C. One GlyDH unit [U] was defined as the amount of enzyme needed to oxidize 1 μmol of glycerol per minute at pH 7 and 25 °C. If indicated, different temperatures and pH values were used.

The values for IC₅₀ (DHA concentration that inhibits 50% GlyDH activity) were determined from nonlinear fit plots using data obtained in experiments in which a fixed concentration of substrate, cofactor, and enzyme were incubated with different DHA concentrations.

Immobilization of the GlyDH

For each immobilization protocol, enzymes were incubated under gentle stirring with different agarose-type supports at the indicated pH and conditions. At different times, samples of supernatant, suspension, and an enzyme solution (blank) incubated under similar conditions but in the absence of the activated support were withdrawn, and the enzyme activities were assayed to evaluate the progress of the immobilization. The immobilized activity is defined as the difference between the blank activity and the supernatant activity at given conditions. Expressed activity is defined as the recovered activity on the solid support after the immobilization process.

Immobilization on monofunctional and heterofunctional glyoxyl supports

Monofunctional glyoxyl supports (Ag-G)

An enzyme solution (4 IU mL⁻¹ of NOX or 1000 IU mL⁻¹ of CAT) was prepared in 100 mM sodium bicarbonate solution at pH 10. Enzyme solution (20 mL) was mixed with Ag-G (2 g) for 3 h. The immobilization was considered to be complete when there was no activity in the supernatant or that supernatant activity was stable for a long time. Afterwards, the suspension was reduced for 30 min at 4 °C with 1 mg mL⁻¹ sodium borohydride.

Heterofunctional glyoxyl supports (Ag-AG)

An enzyme solution (0.4 IU mL⁻¹ of GlyDH-wt, 0.4 IU mL⁻¹ of GlyDH-K97Q) was prepared in 10 mM sodium phosphate buffer solution at pH 7. Enzyme solution (20 mL) was mixed with Ag-AG (2 g) and further incubated at 25 °C. The immobilization was considered to be completed when there was no activity in the supernatant or that supernatant activity was stable for a long time. Then, the preparations were washed with 10 mM phosphate buffer at pH 7, dried under vacuum, and resuspended in sodium bicarbonate solution (20 mL, 10 mM) at pH 10 for 3 h in the presence of 40% PEG. Finally, the preparations were reduced by the addition of 1 mg mL⁻¹ sodium borohydride.

Co-immobilization on Ag-AG supports

Firstly, soluble GlyDH-wt or GlyDH-K97Q (8 IU) in 10 mM sodium phosphate pH 7 was incubated with Ag-AG (2 g). The suspension was stirred gently for 2 h at 25 °C. Once the enzyme was immobilized, the immobilized preparation was collected by filtration. The derivative was incubated in a solution of sodium carbonate (20 mL, 100 mM) and 40% PEG at pH 10.05 that contained CAT (20000 U) for 2 h at 25 °C. After the immobilization of the second enzyme, NOX (8 IU) was added, and the mixture was incubated for 2 h. Then, the resulting immobilized preparation was reduced with 1 mg mL⁻¹ sodium borohydride solution for 30 min at 25 °C. Following the reduction, the solid preparation was equilibrated with 10 mM sodium phosphate at pH 7.

Chemical crosslinking of the enzyme subunits

Dextran (MW = 6000 or 15000–25000 Da) solution was oxidized up to 20 (dxCHO 20% oxide) or 100% (dxCHO 100% oxide) as described previously in Ref. [27]. Briefly, GlyDH, NOX, or CAT immobilized on either Ag-G or Ag-AG (0.7 g) was incubated with dextran (3 mL, 33.33 mg mL⁻¹) at different oxidation grades in 0.2 M sodium phosphate buffer at pH 7 at 4 °C. Samples of the suspension were withdrawn at different times, and the enzyme activity was measured. To stop the crosslinking reaction, the suspension was reduced by raising the pH to 8.5 and by adding 1 mg mL⁻¹ sodium borohydride. This mixture was incubated for 30 min, and the derivative was washed with 10 mM sodium phosphate buffer pH 7.

Inactivation of different GlyDH preparations

Different GlyDH preparations were incubated at 65 °C and pH 7. Samples were withdrawn at different times and the residual activity was measured as described above.

Production of DHA

The reaction mixture was formed by 20 mM glycerol in 100 mM potassium phosphate buffer (pH 7), 150 μM flavin adenine dinucleotide (FAD⁺), and 0.5 mM NAD⁺. The reaction mixture (5 mL) was incubated with NOX (4 IU) and GlyDH (1 IU) at 25 °C. At different times samples were withdrawn, and the DHA amount was determined spectrophotometrically by indirect assay at λ = 630 nm using a solution of 1% of diphenylamine (w/v) in 10% (v/v) sulfuric acid and 90% (v/v) of acetic acid.^[38] The assay was set up for 96-well plates by the addition of 225 μL of diphenylamine solution and 25 μL of sample.

Determination of the efficiency of the elimination of H₂O₂ produced during the enzymatic reaction

The quantification of H₂O₂ production by NOX was performed by a modification of the DAB/HRP method described by Kengen et al.^[39] This method consists of the oxidation of DAB by H₂O₂ in the presence of HRP. Thus, electrons are transferred by HRP from the DAB to the peroxide to yield an insoluble brown product. The calibration curve for H₂O₂ quantification at λ = 460 nm was obtained at six concentration levels, each determined in triplicate. H₂O₂ quantification was performed in two steps. The reaction consisted of the production of H₂O₂ by different preparations of NOX and NOX plus CAT using 0.25 mM NAD⁺ and 5 μM FAD⁺ as substrates. The decrease of the absorbance at λ = 340 nm was moni-

tored spectrophotometrically until the reaction was complete (the absorbance was equal to 0 AU). Immediately after completing the first reaction, 0.47 mM of DAB and 10 μL of 10 mg mL⁻¹ HRP were added. The increase in optical density at λ = 460 nm linked to the oxidation of DAB in the presence of HRP was followed spectrophotometrically. This increase in absorbance was compared to a standard curve, which was prepared separately using known amounts of H₂O₂. Thus, the decrease in NADH in the first assay was related to the amount of H₂O₂ found in the second assay.

Acknowledgements

This work has been supported by the Spanish Ministry of Economy and Innovation (project CTQ2009-07568). We acknowledge COST action CM103-System biocatalysis. We would like to thank IKERBASQUE, Basque foundation for Science for the PhD funding for F.L.-G. We also thank the Comunidad de Madrid government for funding the PhD fellowship for J.R.-M.

Keywords: biotransformations · cofactors · enzyme catalysis · immobilization · protein engineering

- [1] V. Köhler, N. J. Turner, *Chem. Commun.* **2015**, 51, 450–464.
- [2] F. Lopez-Gallego, C. Schmidt-Dannert, *Curr. Opin. Chem. Biol.* **2010**, 14, 174–183.
- [3] W.-D. Fessner, *New Biotechnol.* **2015**, DOI: 10.1016/j.nbt.2014.11.007.
- [4] K. B. Otte, B. Hauer, *Curr. Opin. Biotechnol.* **2015**, 35, 16–22.
- [5] D. Suplatov, V. Voevodin, V. Švedas, *Biotechnol. J.* **2015**, 10, 344–355.
- [6] C. Godoy, B. de Las Rivas, V. Grazú, T. Montes, J. M. Guisán, F. López-Gallego, *Biomacromolecules* **2011**, 12, 1800–1809.
- [7] K. Hernandez, R. Fernandez-Lafuente, *Enzyme Microb. Technol.* **2011**, 48, 107–122.
- [8] C. García-Galan, A. Berenguer-Murcia, R. Fernandez-Lafuente, R. C. Rodrigues, *Adv. Synth. Catal.* **2011**, 353, 2885–2904.
- [9] O. Abian, V. Grazu, J. Hermoso, L. García, R. Fernandez-Lafuente, J. M. Guisán, *Appl. Environ. Microbiol.* **2004**, 70, 1249–1251.
- [10] J. Rocha-Martín, B. de Las Rivas, R. Muñoz, J. M. Guisán, F. López-Gallego, *ChemCatChem* **2012**, 4, 1279–1288.
- [11] S. Schoffelen, J. van Hest, *Soft Matter* **2012**, 8, 1736–1746.
- [12] L. Betancor, H. R. Luckarift, *Biotechnol. Genet. Eng. Rev.* **2010**, 27, 95–114.
- [13] J. Rocha-Martín, S. Velasco-Lozano, J. M. Guisán, F. López-Gallego, *Green Chem.* **2014**, 16, 303–311.
- [14] C. Mateo, J. M. Bolívar, C. Godoy, J. Rocha-Martín, B. C. Pessela, J. A. Curiel, R. Muñoz, J. M. Guisán, G. Fernández-Lorente, *Biomacromolecules* **2010**, 11, 3112–3117.
- [15] J. R. Weiser, P. N. Zawaneh, D. Putnam, *Biomacromolecules* **2011**, 12, 977–986.
- [16] D. Enders, M. Voith, A. Lenzen, *Angew. Chem. Int. Ed.* **2005**, 44, 1304–1325; *Angew. Chem.* **2005**, 117, 1330–1351.
- [17] J. H. Schrittwieser, J. Sattler, V. Resch, F. G. Mutti, W. Kroutil, *Curr. Opin. Chem. Biol.* **2011**, 15, 249–256.
- [18] K. Hernandez, A. Berenguer-Murcia, R. C. Rodrigues, R. Fernandez-Lafuente, *Curr. Org. Chem.* **2012**, 16, 2652–2672.
- [19] S. N. Ruzhenikov, J. Burke, S. Sedelnikova, P. J. Baker, R. Taylor, P. A. Bullock, N. M. Muir, M. G. Gore, D. W. Rice, *Structure* **2001**, 9, 789–802.
- [20] H. J. Hecht, H. Erdmann, H. J. Park, M. Sprinzl, R. D. Schmid, *Nat. Struct. Mol. Biol.* **1995**, 2, 1109–1114.
- [21] I. Fita, M. G. Rossmann, *J. Mol. Biol.* **1985**, 185, 21–37.
- [22] L. Wang, H. Zhang, C.-B. Ching, Y. Chen, R. Jiang, *Appl. Microbiol. Biotechnol.* **2012**, 94, 1233–1241.
- [23] Y. Zhang, F. Gao, S.-P. Zhang, Z.-G. Su, G.-H. Ma, P. Wang, *Bioresour. Technol.* **2011**, 102, 1837–1843.
- [24] V. Maksimović, M. Mojović, Ž. Vučinić, *Carbohydr. Res.* **2006**, 341, 2360–2369.

- [25] L. G. Lee, G. M. Whitesides, *J. Org. Chem.* **1986**, *51*, 25–36.
- [26] R. Daniel, K. Stuert, G. Gottschalk, *J. Bacteriol.* **1995**, *177*, 4392–4401.
- [27] J. Rocha-Martín, A. Acosta, J. Berenguer, J. M. Guisan, F. Lopez-Gallego, *Bioresour. Technol.* **2014**, *170*, 445–453.
- [28] E. Freire, *Proc. Natl. Acad. Sci. USA* **2000**, *97*, 11680–11682.
- [29] D. Kern, E. R. P. Zuiderweg, *Curr. Opin. Struct. Biol.* **2003**, *13*, 748–757.
- [30] L. J. Paine, N. Perry, A. G. Popplewell, M. G. Gore, T. Atkinson, *Biochim. Biophys. Acta Protein Struct. Mol. Enzymol.* **1993**, *1202*, 235–243.
- [31] I. Walsh, G. Minervini, A. Corazza, G. Esposito, S. C. E. Tosatto, F. Fogolari, *Bioinformatics* **2012**, *28*, 2189–2190.
- [32] J. Rocha-Martín, D. Vega, J. M. Bolívar, C. Godoy, A. Hidalgo, J. Berenguer, J. M. Guisán, F. López-Gallego, *BMC Biotechnol.* **2011**, *11*, 101–112.
- [33] L. Betancor, A. Hidalgo, G. Fernández-Lorente, C. Mateo, R. Fernández-Lafuente, J. M. Guisan, *Biotechnol. Prog.* **2003**, *19*, 763–767.
- [34] R. Fernandez-Lafuente, *Enzyme Microb. Technol.* **2009**, *45*, 405–418.
- [35] M. Zheng, S. Zhang, *Biocatal. Biotransform.* **2011**, *29*, 1–10.
- [36] W. Liu, S. Zhang, P. Wang, *J. Biotechnol.* **2009**, *139*, 102–107.
- [37] B. C. C. Pessela, M. Fuentes, C. Mateo, R. Munilla, A. V. Carrascosa, R. Fernandez-Lafuente, J. M. Guisan, *Enzyme Microb. Technol.* **2006**, *39*, 909–915.
- [38] M. Navrátil, J. Tkáč, J. Švitel, B. Danielsson, E. Šturdík, *Process Biochem.* **2001**, *36*, 1045–1052.
- [39] S. W. M. Kengen, J. van der Oost, W. M. de Vos, *Eur. J. Biochem.* **2003**, *270*, 2885–2894.

Received: March 2, 2015

Revised: March 25, 2015

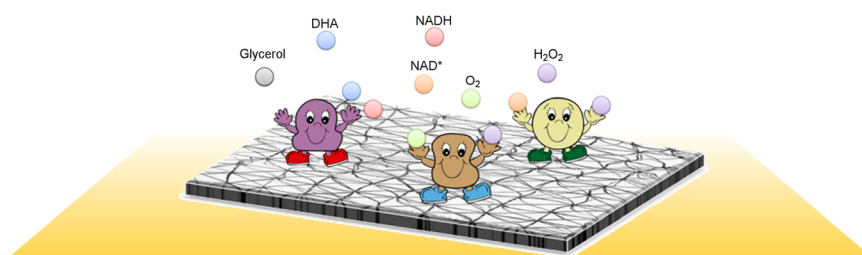
Published online on ■ ■ ■, 0000

FULL PAPERS

J. Rocha-Martin, A. Acosta, J. M. Guisan,*
F. López-Gallego*



Immobilizing Systems Biocatalysis for the Selective Oxidation of Glycerol Coupled to In Situ Cofactor Recycling and Hydrogen Peroxide Elimination



Three's a crowd: The immobilization of three different enzymes on the same carrier surface allows the selective oxi-

dation of glycerol to 1,3-dihydroacetone (DHA) coupled to in situ redox-cofactor recycling and H_2O_2 elimination.